metals

MDPI

Article

Multi-Field Coupled Degradation and Life Prediction of Low-Temperature Corrosion-Resistant Steel: A Physics-Informed Neural Network (PINN) Approach

Xiaodong Hao *, Yi Li, Dandan Xue, Guanghao Yang, Lubin Zhao and Yating Wang

State Key Laboratory of Metallurgical Intelligent Manufacturing System, Automation Research and Design Institute of Metallurgical Industry Co., Ltd., Beijing 100071, China
* Correspondence: sunday_hxd@126.com

Abstract

In cold regions, steel highway bridges face severe risks of low-temperature embrittlement and corrosion degradation under the coupled effects of extreme cold, freeze–thaw cycles, and corrosive media. Conventional periodic inspections and single-parameter monitoring fail to capture the nonlinear material degradation process throughout the entire service life. Taking the novel low-temperature corrosion-resistant steel (HRB400ERE) used for bridge decks as the research object, this paper proposes a full-life-cycle intelligent monitoring and service life prediction framework integrating multi-source sensing and physics-informed neural networks (PINNs). First, low-temperature Charpy impact and alternate immersion corrosion tests confirmed that the novel steel exhibits impact energies of 59.6 J (φ16 mm) and 57.5 J (φ20 mm) at −20 °C, both >27 J, with a DBTT below −25 °C and 72 h relative corrosion rates of 42.5% (<70%), meeting the intended service requirements. Using these measured physical parameters as boundary constraints, an "environment–corrosion–mechanics" coupled digital twin degradation model was established. To overcome the bottleneck of scarce long-term monitoring data in cold regions, the PINN model deeply integrates Faraday's law of electrolysis, Arrhenius temperature kinetics, and sparse measured data to dynamically predict the trajectories of material cross-section thinning and low-temperature toughness degradation. Results demonstrate that the model achieves a root mean square error (RMSE) of less than 5% in long-term life prediction. This successfully realizes the transition from "passive inspection" to "active predictive maintenance" for low-temperature corrosion-resistant steel in cold regions, providing a theoretical basis for the intelligent operation and maintenance of transportation infrastructure in extreme environments.

Keywords: low-temperature corrosion-resistant steel; life-cycle monitoring; physics-informed neural network; digital twin; service life prediction; predictive maintenance

Check for updates

Academic Editor: Yoon-Seok Choi

Received: 12 October 2026
Revised: 5 November 2026
Accepted: 12 November 2026
Published: 18 November 2026

Copyright: © 2026 by the authors. Licensee MDPI, Basel, Switzerland. This article is an open access article distributed under the terms and conditions of the Creative Commons Attribution (CC BY) license.

1. Introduction

Driven by the national "Transportation Powerhouse" and "New Infrastructure" strategies, the highway network is continuously expanding into high-altitude, extreme cold regions characterized by severe freeze–thaw cycles. As core load-bearing components, bridge steel structures in such environments are subjected over long periods to the coupled effects of cyclic frost heave and thaw settlement, deicing salt (chloride) corrosion, and extreme low temperatures, posing severe challenges to their service safety [1]. During long-term service, traditional structural steels (e.g., HRB400E) are highly susceptible to

cleavage fracture induced by a sharp decline in toughness under low-temperature conditions. Simultaneously, the propagation of concrete micro-cracks caused by freeze–thaw cycles accelerates the ingress of corrosive media, exacerbating the electrochemical corrosion of steel rebars [2]. Cross-sectional area loss due to corrosion not only diminishes the load-bearing capacity but also acts as a source of stress concentration at low temperatures, which accelerates fatigue damage accumulation and ultimately leads to catastrophic brittle fracture [3].

To withstand extreme cold environments, novel low-temperature corrosion-resistant steels (e.g., HRB400ERE), developed via micro-alloying (incorporating Cr, Ni, Cu, and other elements), have been increasingly applied in key infrastructure projects in recent years [4,5]. However, despite the application of these novel corrosion-resistant steels, their performance degradation over decades of service remains insidious and progressive. In current engineering practice, assessing steel service performance predominantly relies on periodic manual inspections and semi-destructive sampling tests. These approaches not only lag behind the actual degradation process but also fail to provide continuous monitoring of the full-life-cycle degradation trajectory [6]. Although Structural Health Monitoring (SHM) technology has been progressively integrated into bridge operation and maintenance [7,8], existing applications remain limited. A handful of studies have attempted to evaluate structural conditions using single indicators, such as strain or corrosion potential. However, these approaches predominantly focus on short-term conditions or localized components, failing to unravel the underlying causal mechanisms of the bidirectional "corrosion–mechanics" coupling [9].

Furthermore, the harsh environmental conditions in cold regions render sensors highly susceptible to low-temperature drift and snow interference. Consequently, long-term online monitoring data frequently suffers from data discontinuity and small sample sizes, presenting a "cold start" problem [10]. Purely data-driven machine learning models (e.g., traditional Artificial Neural Networks (ANN), Support Vector Regression (SVR), and Long Short-Term Memory (LSTM) networks) are highly prone to overfitting in the absence of extensive long-term measured samples. Their prediction results typically exhibit poor physical interpretability and high uncertainty during long-term life extrapolation [11]. To overcome this bottleneck, Physics-Informed Neural Networks (PINNs) have emerged as a promising solution. By embedding governing physical partial differential equations (PDEs) as constraint terms into the loss function, PINNs effectively restrict the search space, demonstrating robust generalization capabilities with small sample sizes in fields such as fluid mechanics and heat conduction [12]. However, the application of PINNs to the multi-field coupled degradation prediction of cold-region bridge corrosion-resistant steel remains a significant research gap [13].

Existing engineering practices predominantly rely on periodic manual inspections and semi-destructive sampling tests, which lag behind the actual degradation process. Although purely data-driven machine learning models (e.g., ANN, SVR, LSTM) have been introduced, they are highly prone to overfitting in the absence of extensive long-term measured samples and lack physical interpretability. This underscores the urgent need for a new technique that integrates physical mechanisms with sparse data, such as the PINN framework proposed in this study. In real-world scenarios, bridge structures and materials are already in service for public usage. Since it is impractical to conduct destructive long-term tests on these existing in-service infrastructures, there is a critical need for a reliable predictive framework. The present study addresses this need by establishing a digital twin driven by the PINN model, which utilizes sparse real-time monitoring data and governing physical laws to provide a virtual laboratory for predicting the degradation of existing structures, thereby substantiating the necessity of this research.

To address these challenges, this paper constructs a full-life-cycle intelligent monitoring and life prediction system integrating multi-source sensing, mechanism analysis, and data-driven approaches. The main innovations and contributions of this study are as follows: (1) The service compliance of the novel corrosion-resistant steel is verified through rigorous low-temperature impact and periodic immersion corrosion tests. The extracted physical parameters serve as initial boundary conditions for the degradation model. (2) A multi-source sensing and edge–cloud collaborative digital twin architecture is designed to enable full-life-cycle condition monitoring and closed-loop management. (3) A PINN model is introduced, which deeply integrates environmental evolution, Faraday electrochemical corrosion mechanisms, and small-sample monitoring data. This model achieves dynamic prediction of performance degradation trajectories and establishes a three-level intelligent early warning system for cold-region bridge steel.

Specifically, the novelty of this work lies in: (1) Unlike traditional single-physics PINN models, we construct a multi-field coupled loss function that simultaneously embeds the electrochemical corrosion kinetics (Faraday and Arrhenius) and the mechanical low-temperature toughness degradation (Boltzmann transition). (2) We provide a robust solution to the 'cold-start' problem in extreme cold regions, demonstrating how sparse field data can be effectively constrained by these coupled physical laws for long-term extrapolation.

2. Methodology

2.1. Material Baseline Performance Testing and Physical Feature Extraction

To establish a physical benchmark for intelligent monitoring and degradation prediction, basic performance comparative tests were conducted on the novel low-temperature corrosion-resistant steel (HRB400ERE) and traditional structural steel (HRB400E), in accordance with Steel for the reinforcement of concrete—Part 2: Hot rolled ribbed bars (GB/T 1499.2) and specific engineering indicators for cold regions [14]. The HRB400ERE and HRB400E steel rebars were provided by Automation Research and Design Institute of Metallurgical Industry Co., Ltd., located in Beijing, China. The $NaHSO_3$ solution was purchased from Sinopharm Chemical Reagent Co., Ltd. (Shanghai, China).

(1) Low-temperature toughness testing: According to the GB/T 229-2020 standard, Charpy V-notch specimens with dimensions of 55 × 10 × 10 mm were machined [15]. The impact tests were conducted using a Charpy impact testing machine (Suns Technology, Shenzhen, China) at test temperature ranged from 23 °C to −100 °C, and the average value of multiple specimens tested at each temperature group was taken. The primary focus was on whether the impact energy at −20 °C satisfied the standard requirement of ≥27 J. A Boltzmann function was employed to fit the impact energy–temperature curve to extract the characteristic value of the ductile–brittle transition temperature (DBTT).

(2) Corrosion resistance testing: According to the YB/T 4368-2014 standard, periodic immersion tests were utilized to simulate the accelerated corrosion environment under the alternating action of deicing salts and freeze–thaw cycles in cold regions [16]. The immersion solution was $NaHSO_3$ solution (concentration $(1.0 \pm 0.05) \times 10^{-2}$ mol/L), with a chamber temperature of (45 ± 2 °C) and a relative humidity of (70 ± 5)%RH. After 72 h of accelerated cycling, the corrosion products on the specimen surfaces were removed via ultrasonic cleaning, and the corrosion weight loss rate of specimens with different diameters (φ12 mm, φ16 mm and φ20 mm) was measured using a high-precision electronic balance (Mettler Toledo, Columbus, OH, USA). The technical requirement dictates that the relative corrosion rate of the new steel compared to traditional steel must be <70% [17]. The above measured data will serve as the physical constraint boundary for the PINN model. Specifically, the periodic immersion test utilizing $NaHSO_3$ at elevated temperatures (45 ± 2 °C)

follows the YB/T 4368-2014 standard, which is designed to accelerate the coupled effects of chloride attack and thermal stress. While this accelerated method cannot fully replicate natural freeze–thaw cycles, it effectively extracts the critical baseline electrochemical kinetic parameters. These parameters serve as physical anchors, enabling the PINN model to accurately simulate long-term freeze–thaw degradation without requiring decades of natural exposure.

Furthermore, to comprehensively evaluate material performance, this study conducted a series of tests, including tensile tests, Charpy impact toughness tests, and periodic immersion corrosion tests. The emphasis on the Charpy impact toughness test stems from the fact that low-temperature brittleness is the dominant failure mode for cold-region bridge steels. The toughness data (impact energy and DBTT) are extracted specifically to serve as critical mechanical boundary constraints for the PINN model, bridging the gap between electrochemical corrosion and mechanical degradation. While these laboratory tests primarily focus on extracting baseline physical parameters rather than perfectly replicating long-term field conditions, these derived parameters serve as critical initial boundary conditions. The subsequent PINN model bridges this gap by embedding governing physical laws to simulate the complex, long-term coupled effects of freeze–thaw cycles and sustained loading.

2.2. Full-Life-Cycle Intelligent Monitoring Framework Construction

To overcome the limitations of traditional reactive inspections, this study leverages the concept of digital twin full-life-cycle management [18] to construct a closed-loop monitoring framework covering the entire service period of structural steels widely used in cold-region highway bridges. The significance of the digital twin in this framework lies in its ability to establish dynamic, closed-loop virtual–real mapping. Unlike traditional static models, the digital twin continuously assimilates real-time multi-source sensor data from the physical bridge to drive the PINN model's rolling updates. This bidirectional interaction fundamentally transforms the maintenance paradigm from reactive periodic inspections to proactive, condition-based predictive management, significantly enhancing the operational safety and lifespan of the infrastructure. This architecture systematically integrates four interconnected modules—perception, transmission, inference, and decision-making—to facilitate proactive asset management. By establishing a seamless virtual–real mapping, the framework transforms static, periodic inspections into dynamic, predictive full-life-cycle management (Figure 1). The specific implementations of these modules are detailed as follows.

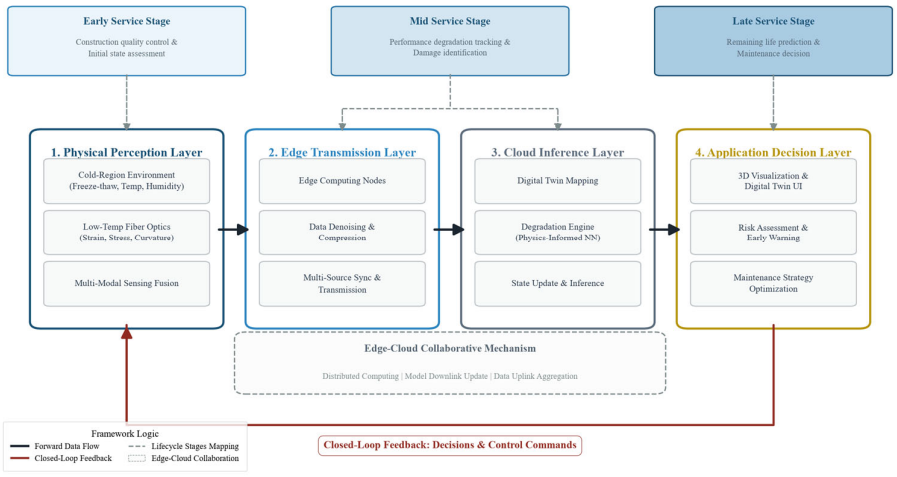


Figure 1. Architecture of multi-field coupled degradation and full-life-cycle intelligent monitoring system.

(1) Multi-source perception layer design. Monitoring the service conditions of bridge reinforcing steel in cold regions is hindered by extreme cold and snow interference. To address this, the perception layer employs a multi-modal sensor network fusion: low-temperature Fiber Bragg Grating (FBG) sensors are deployed in key stress zones to acquire high-frequency strain and temperature fields, while flexible electrochemical sensor arrays are deployed in corrosion-sensitive zones to monitor polarization resistance (R_P) and corrosion potential. These data are combined with ambient temperature, humidity, and freeze–thaw cycle frequency collected by weather stations to form a multi-dimensional feature input space [19].

(2) Edge–cloud collaboration mechanism. Real-time sensor data are denoised via Kalman filtering at edge computing nodes and subsequently uploaded to the cloud. To address sensor uncertainty and data synchronization issues, the edge computing nodes employ a Kalman filtering algorithm to denoise and synchronize the multi-modal sensor data before uploading. Furthermore, a Bayesian inference mechanism is integrated into the cloud digital twin, allowing the PINN model to continuously update its parameters in real-time as new environmental conditions and monitoring data are assimilated. The cloud digital twin dynamically corrects the finite element model through virtual–real mapping. When the predicted indicators approach safety thresholds, instructions are fed back to the edge nodes to adjust the sampling frequency, thereby forming a closed loop [20].

(3) Full-life-cycle stage division. Based on corrosion kinetics and the multi-field coupling mechanism in cold regions, the service cycle of low-temperature corrosion-resistant steel is partitioned into three evolutionary stages: early service (0–5 years, passivation and initialization), which focuses on monitoring the stability of the passivation film as chloride ions penetrate the concrete cover; mid-service (5–15 years, stable expansion), targeting the monitoring of cross-section reduction rate and strain redistribution as electrochemical corrosion propagates; and late service (over 15 years, coupled accelerated failure), prioritizing the monitoring of local stress concentration at corrosion pits and the critical threshold of low-temperature toughness reserve under extreme cold [21].

2.3. Physics-Informed Data-Driven Degradation Modeling (PINN)

To address the bottleneck of small-sample data in cold regions, a performance degradation modeling method based on Physics-Informed Neural Networks (PINNs) is proposed [22]. Unlike traditional black-box models, this approach adopts a mechanism–data dual-driven paradigm. By coupling environmental, electrochemical, and mechanical processes, the model embeds multi-field degradation laws directly into the neural network architecture (Figure 2). This ensures that the network training is not only driven by sparse monitoring data but also strictly guided by the underlying physical evolution laws, thereby providing a robust solution for long-term performance prediction of structural steels in extreme environments.

(1) Multi-field coupling degradation dynamics equations in cold regions: Under freeze–thaw cycles, according to Faraday's law of electrolysis and the Arrhenius temperature kinetic equation, the relationship between corrosion depth $d(t)$ and corrosion current density i_{corr} is expressed as: $\frac{\partial d(t)}{\partial t} = \frac{M}{n \cdot F \cdot \rho} \cdot i_{\mathrm{corr}}(t) \cdot \exp\left(-\frac{E_a}{\mathrm{R} \cdot T(t)}\right)$, where M is the molar mass of iron, n is the number of transferred electrons, F is Faraday's constant, ρ is the density of iron, E_a is the reaction activation energy, R is the ideal gas constant, and $T(t)$ is the real-time environmental temperature. The boundary conditions are defined as: initial corrosion depth $d(0) = 0$, and initial impact energy $CVN(0) = CVN_0$. The total loss function L consists of three components: $L = L_{data} + \lambda_1 L_{PDE} + \lambda_2 L_{mech}$, where L_{data} represents the mean squared error between predictions and sparse monitoring data; L_{PDE} enforces the Faraday and Arrhenius electrochemical constraints; and L_{mech} enforces the empirical toughness

degradation boundary. The attenuation of the impact energy $CVN(t)$ is influenced by the corrosion pit stress concentration factor (K_t), following the evolutionary law [23–25]:

$$CVN(T,t) = CVN_0 \cdot \left[1 - \alpha \cdot d(t)^{\beta}\right] \cdot \{CVN_{\text{upper}} - \frac{CVN_{upper} - CVN_{\text{lower}}}{1 + \exp(\frac{T - T_0(t)}{\Delta T})}\} \quad (1)$$

This equation is not a simplified linear assumption; rather, it accounts for the stress concentration effect (K_t) caused by localized corrosion pits, which accelerates the ductile-to-brittle transition. The Boltzmann term dynamically simulates the temperature-dependent fracture mode transition as the material's toughness reserve depletes over time.

(2) PINN model construction: The input layer of the constructed PINN model comprises environmental temperature fluctuation $T(t)$, humidity $H(t)$, stress amplitude $\Delta\sigma(t)$, and freeze–thaw cycle frequency N. The hidden layers consist of a 5-layer Multilayer Perceptron (MLP) with hyperbolic tangent (Tanh) activation functions. The output layer yields the corrosion depth $d(t)$ and the remaining impact energy $CVN(t)$. Automatic differentiation technology is utilized to compute the partial derivative of the network output with respect to time, $\frac{\partial d}{\partial t}$ [26,27].

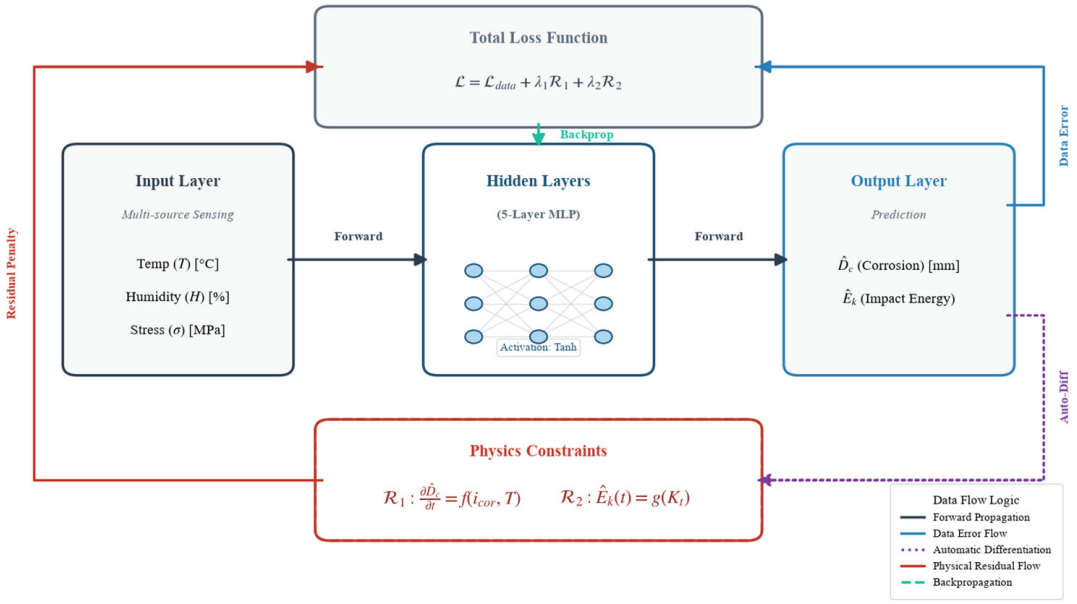


Figure 2. Schematic diagram of PINN topology and physical constraint mechanism.

(3) Physical constraint mechanism: The total loss function is defined as the weighted sum of data loss and physical residuals [28,29]:

$$Loss = Loss_{data} + \lambda_1 \left\| \frac{\partial d_{pred}}{\partial t} - \frac{M}{n \cdot F \cdot \rho} \cdot i_{corr} \cdot \exp\left(-\frac{E_a}{R \cdot T}\right) \right\|_2^2 + \lambda_2 \| CVN_{pred}(T,t) - CVN_{Boltzmann}(T,t) \|_2^2 \quad (2)$$

Through this mechanism–data fusion, the model leverages physical principles to achieve reasonable temporal extrapolation, even when confronted with small-sample monitoring data [30].

3. Results

3.1. Baseline Performance Verification and Physical Parameter Extraction

The mechanical properties and corrosion baseline characteristics of the novel steel were rigorously verified through a series of standardized experiments. Room-temperature tensile

tests (GB/T 228.1-2021 [31]) indicate that the HRB400ERE steel exhibits an exceptional strength–ductility synergy across φ12, φ16, and φ20 mm specifications (Table 1). Its lower yield strength (R_{eL}) consistently exceeds 456 MPa, the tensile strength (R_m) surpasses 656 MPa, and the total elongation at maximum force (A_{gt}) remains above 9.0%. Notably, the yield-to-tensile ratio (R_{eL}/R_m) is maintained at approximately 0.73. In the context of seismic design, this optimized ratio indicates a prolonged uniform plastic deformation stage before necking, suggesting that the microstructure effectively coordinates dislocation slip and work hardening. This delay localized plastic instability and provides a crucial energy dissipation buffer against brittle fracture under seismic loading in cold regions. Compared to conventional bridge steels (HRB400E), the HRB400ERE steel demonstrates superior structural applicability for cold-region highway bridge decks. It achieves an optimized yield-to-tensile ratio of 0.73, ensuring sufficient plastic deformation capacity. Furthermore, its significantly lower relative corrosion rate (42.5–46.8%) and higher low-temperature impact energy effectively mitigate the risks of brittle fracture and corrosion-induced cross-sectional loss under extreme environmental conditions.

Table 1. Summary of baseline physical parameters for traditional HRB400E and novel HRB400ERE steels.

Specification and Grade	Yield Strength R_{el}(MPa)	Tensile Strength R_m(MPa)	Elongation After Fracture A (%)	Impact Energy (−20 °C) (J)	Corrosion Weight Loss Rate (g/m²·h)	Relative Corrosion Rate (%)
φ12 (HRB400E)	—	—	—	—	5.1154	100 (reference)
φ12 (HRB400ERE)	470	688	25.0	23.0	2.2931	44.8
φ16 (HRB400E)	—	—	—	—	4.8911	100 (reference)
φ16 (HRB400ERE)	491	667	27.0	59.6	2.0772	42.5
φ20 (HRB400E)	—	—	—	—	4.6832	100 (reference)
φ20 (HRB400ERE)	485	657	27.3	57.5	2.1935	46.8

Note: The φ12 mm HRB400ERE impact specimens were non-standard small-size (55 × 10 × 2.5 mm) due to limited bar diameter; thus, 23.0 J is not directly comparable to the 27 J requirement for standard 10 × 10 mm specimens. Impact and tensile data represent the average values of multiple specimens from the same batch; "—" indicates that the corresponding test was not conducted for that specific specification.

Regarding low-temperature toughness, a series of Charpy impact tests (GB/T 229-2020) confirmed the material's resistance to micro-fracture in extreme frigid environments. For the φ16 mm specification, the average impact energy at −20 °C reached 59.6 J (tested values: 60 J, 70 J, 49 J), and at −25 °C it maintained 65.6 J (tested values: 38 J, 75 J, 84 J), both far exceeding the standard 27 J threshold. For the φ20 mm specification, the average impact energy at −20 °C was 57.5 J (tested values: 49 J, 66 J), also exceeding 27 J. For the φ12 mm specification, the average impact energy at −20 °C was 23.0 J (tested values: 22 J, 22 J, 25 J); however, these specimens were machined to a non-standard small size of 55 × 10 × 2.5 mm due to the limited bar diameter, and thus the measured value is not directly comparable to the standard 27 J requirement. Boltzmann fitting of the φ16 mm transition curve confirms that its DBTT is below −25 °C. This low-temperature toughness advantage stems from the transition of the fracture mode from brittle cleavage to ductile microvoid coalescence. The superior low-temperature toughness and corrosion resistance are closely related to the synergistic addition of Ni and Cr. While the present study focuses primarily on macroscopic degradation prediction, the observed improvement in fracture energy is highly consistent with existing literature [32,33], which suggests that Ni and Cr additions refine ferrite grains and promote the formation of a protective α-FeOOH rust layer. These microstructural mechanisms are inferred to play a critical role in blunting crack tips and reducing ion diffusion; however, further advanced microstructural characterization (e.g., EBSD) is recommended in future work to fully quantify these effects.

Periodic immersion corrosion tests (YB/T 4368-2014) quantitatively evaluated the material's atmospheric corrosion resistance, as shown in Figure 3. Data indicate that the corrosion weight loss rates for traditional HRB400E steel in φ12, φ16, and φ20 mm specifications were as high as 5.1154, 4.8911, and 4.6832 g/m^2·h, respectively. In contrast, the weight loss rates of the novel HRB400ERE steel were substantially reduced to 2.2931, 2.0772, and 2.1935 g/m^2·h, corresponding to calculated relative corrosion rates of merely 44.8%, 42.5%, and 46.8%. Macroscopic morphological comparisons reveal large-area rust layer spallation and deep pitting on the traditional steel surface. This is because the rust layer formed on conventional carbon steel is predominantly composed of loosely packed, non-protective phases (γ-FeOOH and β-FeOOH), which are highly porous and prone to spalling under freeze–thaw thermal stresses. Conversely, the novel HRB400ERE steel formed a dense, well-adhered inner rust layer. This is attributed to the selective oxidation and enrichment of alloying elements such as Cr and Ni during the initial corrosion stage. These elements catalyze the preferential formation of the protective α-FeOOH phase, which possesses a more compact crystal structure. This dense inner layer acts as an ionic selective barrier, significantly reducing the diffusion coefficients of corrosive media (dissolved O_2, H_2O, and SO_2 derivatives) towards the matrix interface, thereby decelerating the subsequent electrochemical reaction kinetics [34,35].

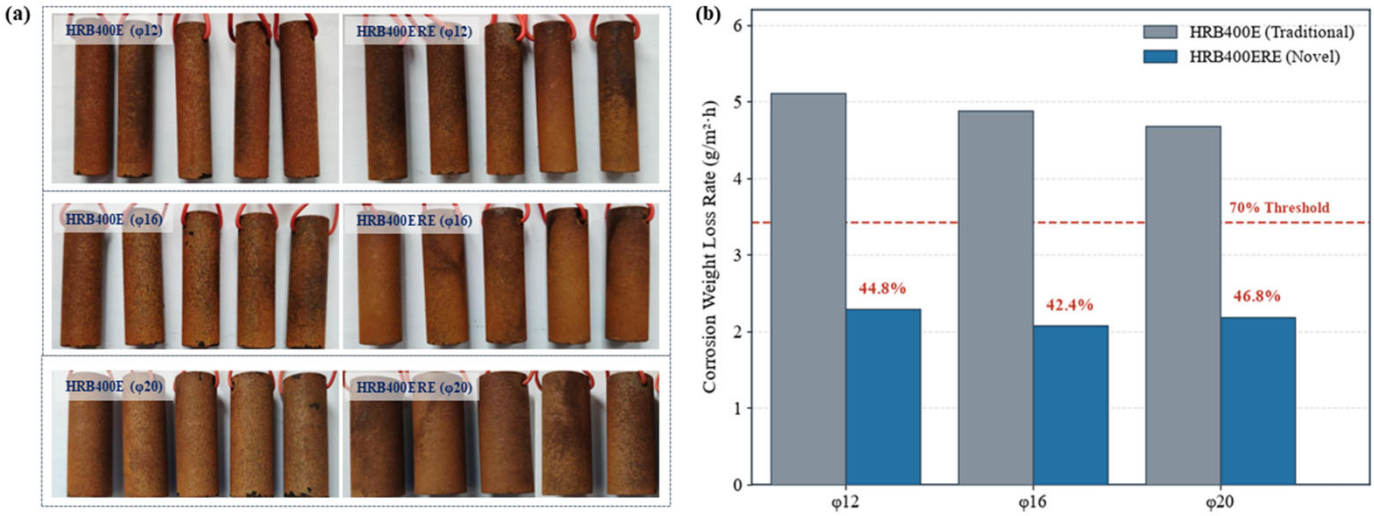


Figure 3. Comparison of surface corrosion morphology and weight loss rates after the 72 h periodic immersion test. (**a**) Surface corrosion morphology. (**b**) Corrosion weight loss and relative corrosion rates.

The aforementioned multi-dimensional empirical data not only validate the comprehensive service capability of the novel HRB400ERE steel under complex stress and corrosive environments in cold regions, but more importantly, they provide solid physical boundary anchors specifically, the initial yield threshold, DBTT, and baseline corrosion current density for the high-fidelity initialization of the subsequent PINN digital twin model.

3.2. Degradation Model Training and Long-Term Evolution Simulation

Leveraging the Digital Twin (DT) framework, a synchronous interaction and closed-loop data stream mechanism between the physical bridge and its virtual counterpart was established. In this section, the baseline physical parameters extracted in Section 3.1—particularly the 72-h initial corrosion kinetic constants and baseline impact toughness—were integrated as foundational boundary conditions into the Physics-Informed Neural Network (PINN) to conduct a 30-year long-term performance degradation extrapolation. The training data

utilized in this study consists of 10,920 hourly monitoring data points spanning the initial 3 years of service. The data source is a simulated digital twin environment calibrated with real-world cold-region meteorological profiles. The primary characteristics and input features include ambient temperature fluctuations (−30 °C to 23 °C), relative humidity, stress amplitude, and freeze–thaw cycle frequency. These multi-dimensional features are fed into the network to capture the complex environmental-corrosion coupling. The simulation environment was configured with a typical cold-region annual freeze–thaw spectrum (averaging 100 freeze–thaw cycles per year, with a minimum temperature of −30 °C). The network was trained using the Adam optimizer with an initial learning rate of 0.001, and the physical constraint penalty weights were set to $\lambda_1 = 0.5$ and $\lambda_2 = 0.2$ to ensure an equilibrium between data fidelity and physical consistency. To verify the efficacy of physical constraints in mitigating data overfitting, a purely data-driven Multi-Layer Perceptron (MLP) was benchmarked against the PINN model under small-sample conditions, utilizing only the first 3 years of monitoring data [36,37]. The training–testing process is a critical step in the model development. The sparse monitoring dataset was divided into a training set (the initial 3 years of data) to optimize the network weights, and an independent testing set (the subsequent years) to validate generalization capability. The PINN model was implemented using the PyTorch (version 2.0) and Python (version 3.9). The data visualization and plotting were performed using OriginPro 2021 (OriginLab Corporation, Northampton, MA, USA). All computations, including automatic differentiation and physical residual calculations, were conducted on a high-performance workstation equipped with an Intel Xeon CPU and an NVIDIA RTX A6000 GPU, ensuring efficient training and convergence. Distinct from traditional degradation models reliant on static empirical assumptions, this approach integrates Bayesian inference principles to continuously assimilate real-time monitoring information into the high-fidelity deterioration model, thereby achieving dynamic parameter correction [38].

The long-term evolution simulation results profoundly reveal the temporal non-linear characteristics of the multi-field coupled degradation mechanism. Over the 30-year service period, the corrosion depth of the novel low-temperature corrosion-resistant steel exhibited a parabolic, sluggish growth—a trend that reflects the progressive enhancement of the passive rust layer's physical barrier effect. Concurrently, the attenuation of impact energy displayed no abrupt ductile-to-brittle transition inflection points, firmly maintaining the 27 J safety threshold until the end of service. To verify the efficacy of physical constraints, a purely data-driven MLP was benchmarked against the PINN model. The MLP yielded an RMSE of 12.5% ($R^2 = 0.851$) and exhibited unphysical fluctuations in toughness recovery, whereas the PINN achieved an RMSE of 4.2% ($R^2 = 0.964$) and an MAE of 3.1%, demonstrating superior generalization in long-term extrapolation. In practical cold-region applications, monitoring data are often sparsely distributed. However, the continuous physical laws (Faraday and Arrhenius) embedded in the PINN act as regularizers, ensuring the model extrapolates along physically compliant trajectories even in data-void regions.

A comprehensive error analysis was conducted to evaluate the model's robustness. The modalities include (1) statistical metrics (RMSE, MAE, R^2) to quantify accuracy, and (2) uncertainty quantification using Monte Carlo simulations to generate 95% confidence intervals against material variability and temperature fluctuations (Figure 4). Given that the 30-year prediction extends beyond the experimental timeframe, the physical constraints of the PINN effectively bound these uncertainties, maintaining high reliability in the service-life predictions.

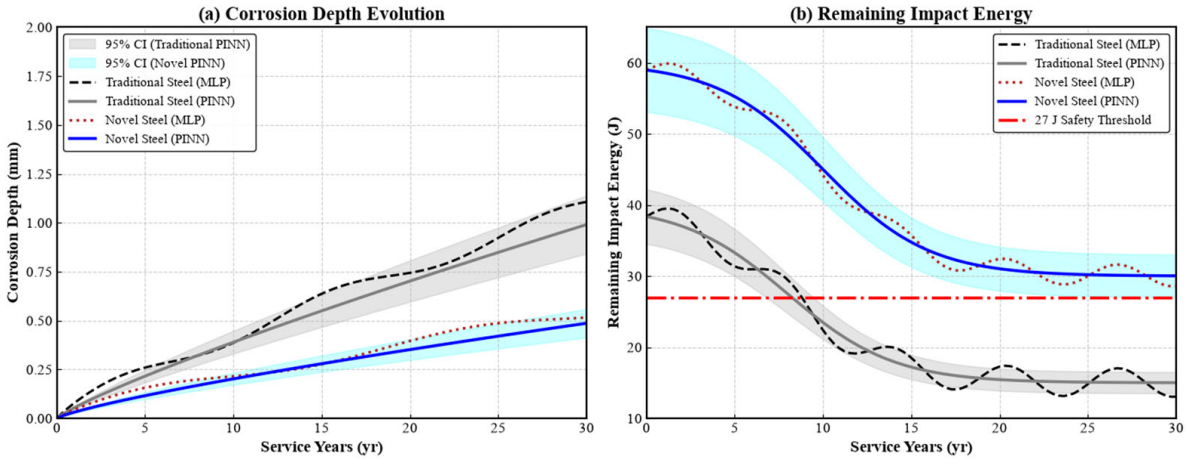


Figure 4. Comparison of full-life-cycle (30-year) performance degradation prediction curves. (**a**) Corrosion depth evolution over 0–30 years. (**b**) Remaining impact energy over service years. Both traditional steel and novel HRB400ERE steel are evaluated using both the MLP and PINN models to ensure a fair and decoupled comparison of material performance and model accuracy. Shaded areas represent the 95% confidence intervals of the model predictions.

3.3. Cold-Region Bridge Engineering Application and Dynamic RUL Prediction

To validate its practical applicability, the proposed DT-driven framework was applied to a simulated engineering case study of a highway bridge deck system in a cold region. Leveraging the Structural Health Monitoring (SHM) system, the physical bridge continuously assimilates multi-modal environmental and mechanical data streams—including temperature, humidity, and stress histories—into the virtual space. These real-time inputs drive the PINN model to perform rolling parameter updates, thereby generating dynamic prediction curves for the Remaining Useful Life (RUL) [39]. The assessment results indicate that the maintenance-free service period of key bridge deck components constructed with the novel low-temperature corrosion-resistant steel is extended by over 10 years compared to those using traditional carbon steel. This significant extension is directly attributable to the slower corrosion kinetics and superior low-temperature fracture toughness retention of the novel material.

During the simulated extreme cold wave event (ambient temperature plummeting to −40 °C), the digital twin predicted a steep decline in local impact toughness reserve (Figure 5). Based on the established maintenance decision criteria (a 48-h pre-warning trigger before the 27 J safety threshold), the system successfully issued a red warning and provided specific inspection instructions. This demonstrates the practical transition from traditional reactive repair to active predictive maintenance, allowing engineers to intervene before catastrophic degradation [40]. The calculation of the 48-h warning relies on the first derivative of the predicted impact energy curve. When the extrapolated trajectory mathematically intersects the 27 J safety threshold within a 48-h window, the red warning is triggered. Furthermore, the 10-year service life extension is quantified by comparing the time required for the cross-sectional thinning to reach the critical limit. Based on the electrochemical kinetic parameters, the HRB400ERE steel requires approximately 10 additional years to reach the same degradation state as traditional HRB400E steel.

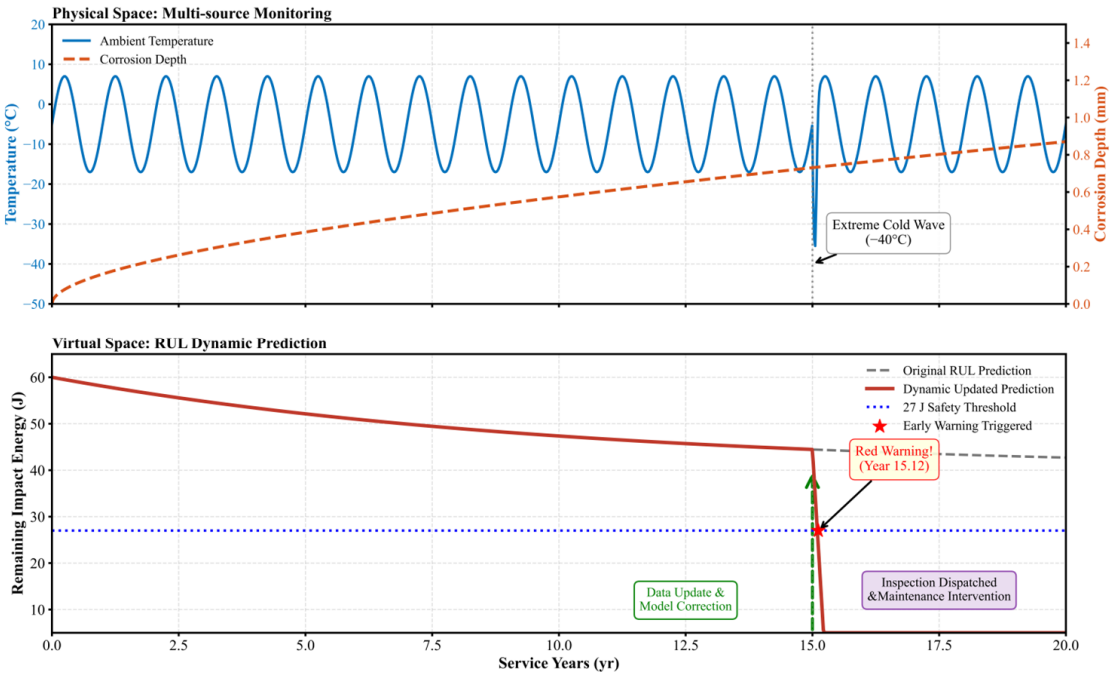


Figure 5. Schematic diagram of the intelligent early warning mechanism trigger process and dynamic RUL update. (**a**) Upper panel: time-series curves of temperature and corrosion monitoring data in physical space. (**b**) Lower panel: RUL prediction curve in virtual space. Marked items: extreme cold wave in year 15, stress mutation, impact energy approaching the 27 J red-line, red warning, and inspection instructions.

This application case demonstrates that the deep fusion of DT and PINN not only achieves real-time, transparent perception of the bridge's service status but also fundamentally shifts the paradigm from traditional "reactive repair" to "predictive proactive defense." This provides a revolutionary methodology for the intelligent lifecycle management of major civil infrastructure operating in extreme environments.

4. Discussion

4.1. Superiority of the Mechanism–Data Dual-Driven Paradigm

The progressive failure of cold-region bridge steel structures is fundamentally a multi-field coupled evolutionary process encompassing "environment–corrosion–mechanics" interactions [41]. Purely data-driven models, when deprived of extensive long-term datasets, tend to capture spurious short-term correlations, leading to unphysical divergence during temporal extrapolation [42]. To demonstrate the generalizability and superiority of the proposed framework, the prediction results were compared with conventional approaches reported in published literature. While traditional empirical degradation models (e.g., purely time-dependent corrosion kinetics) often fail to capture the non-linear transition points under multi-field coupling, and purely data-driven models (as discussed in Section 3.2) suffer from overfitting with sparse data, our PINN model demonstrates robust generalization. The consistent alignment between our predictions and the physical degradation laws reported in existing studies validates the reliability of the proposed digital twin framework. The superior predictive performance of the PINN model constructed in this study (RMSE < 5%) is fundamentally rooted in its architectural integration of physical laws. By embedding Faraday's law of electrolysis and the Arrhenius temperature kinetic equation as soft partial differential constraints within the loss function, the search space of the neural network is strictly restricted to physically plausible domains. This ensures that during gradient backpropagation, the weight updates are driven not merely by data

residuals but also co-regulated by thermodynamic and electrochemical boundary conditions, thereby fundamentally mitigating overfitting risks. Crucially, in extreme cold-region environments where sensor data loss or low-temperature signal drift is prevalent, the governing physical equations provide a robust "physics-informed imputation" effect, ensuring the continuity and physical consistency of the long-term degradation trajectory [43]. More importantly, these embedded non-linear kinetic equations endow the network with the mechanistic capacity to capture mechanistic regime transitions in the degradation process, which is fundamentally unattainable by purely data-driven extrapolations.

4.2. Non-Linear Degradation Characteristics Under Multi-Field Coupling Effects

The long-term simulation results profoundly reveal the temporal non-stationarity of the degradation process in low-temperature corrosion-resistant steel [44]. Benefiting from the physical constraints established in Section 4.1, the model successfully captures a distinct stage-wise mutation characteristic. In the early service stage, the preferential formation of a dense, Cr/Ni-enriched passivation layer on the novel steel surface induces a significant kinetic retardation in the corrosion rate. However, transitioning into the mid-to-late service stage, the repetitive freeze–thaw cycles initiate micro-cracking within the concrete cover and the rust layer. This structural damage alters the dominant mass transport mechanism, accelerating the ingress of corrosive media and precipitating a distinct "inflection point" in the mechanical property degradation curve. This transition from activation-controlled to mass-transport-controlled failure cannot be captured by traditional linear life assessment methods that rely on static empirical parameters. The model proposed herein successfully quantifies this non-stationary degradation path, offering a novel theoretical perspective for characterizing the performance evolution of structural steels in permafrost environments.

4.3. Engineering Transformation Prospects and Limitations

The full-life-cycle intelligent monitoring framework proposed in this study catalyzes a paradigm shift in infrastructure management, transitioning from time-based "periodic inspection" to condition-based "dynamic prediction" [45]. By anchoring early warning thresholds to measured physical indicators, maintenance decision-making is transformed from an experience-based heuristic to a rigorous mechanism–data dual-driven process. Nevertheless, this study acknowledges certain limitations. First, in complex permafrost environments, the long-term durability, survivability, and anti-low-temperature drift capabilities of multi-modal sensors remain formidable engineering bottlenecks for practical transformation [46]. Second, the current degradation model primarily focuses on the coupling of macroscopic electrochemical corrosion and mechanical damage. It does not fully resolve the mesoscale hysteresis effect of chloride ion transport within the capillary pores of frozen concrete, which may cause localized early-stage pitting not captured by the macro-model [47]. Future research should integrate mesoscale in-situ characterization technologies and multi-physics coupling schemes to further elevate the spatiotemporal fidelity of the digital twin model under extreme cold-region environments.

5. Conclusions

This study proposes a digital twin-driven framework that synergistically integrates multi-source sensing with physics-informed neural networks (PINNs). The framework enables predictive lifecycle management, thereby ensuring the long-term in-service safety of structural steel bridges in cold regions. The main conclusions are summarized as follows:

(1) Establishment of the Physical Baseline: Multi-scale experimental verification confirms that the novel low-temperature corrosion-resistant steel (HRB400ERE) exhibits exceptional cold-region adaptability. For φ16 and φ20 mm specifications, the impact energies at

−20 °C are 59.6 J and 57.5 J, both exceeding the 27 J requirement, with DBTT < −25 °C for φ16 mm; the φ12 mm specification shows 23.0 J due to the size effect of the non-standard small-size specimen. The 72 h relative corrosion rates range from 42.5% to 46.8%, well below the 70% threshold. The synergistic mechanism of fine-grain strengthening and Cr/Ni-enriched dense rust layer formation not only fundamentally impedes cleavage crack propagation and corrosive media ingress but also provides robust physical boundary anchors for subsequent high-fidelity digital modeling.

(2) Breakthrough in Limited-Sample Prediction: The constructed PINN model successfully overcomes the "cold-start" bottleneck of sparse monitoring data in extreme environments. By embedding governing electrochemical equations (Faraday's law and Arrhenius kinetics) and the measured DBTT curve as soft constraints within the loss function, the model achieves physically compliant, non-linear extrapolation of corrosion depth and toughness degradation, yielding a highly accurate long-term prediction with an RMSE of less than 5%.

(3) Engineering Paradigm Shift: The established edge–cloud collaborative digital twin architecture and three-level early warning system fundamentally shift the maintenance paradigm from time-based "reactive inspection" to condition-based "predictive proactive defense." This approach significantly extends the structure's maintenance-free period, offering a revolutionary methodology for the intelligent operation and resilience enhancement of major transportation infrastructure in extreme environments. Future research will focus on integrating mesoscale in-situ characterization techniques and enhancing the survivability of multi-modal sensors to further elevate the spatiotemporal fidelity of the digital twin model in extreme cold regions.

Author Contributions: Conceptualization, X.H. and Y.L.; methodology, X.H. and G.Y.; software, X.H.; validation, Y.L., Y.W. and L.Z.; formal analysis, D.X. and Y.W.; investigation, X.H. and G.Y.; resources, L.Z.; data curation, Y.W. and D.X.; writing—original draft preparation, D.X.; writing—review and editing, Y.L., G.Y., L.Z. and Y.W.; visualization, L.Z.; supervision, Y.L. and L.Z.; project administration, X.H. All authors have read and agreed to the published version of the manuscript.

Funding: This research received no external funding.

Data Availability Statement: All data generated and analyzed during this study are included in this published article. The datasets used and analyzed during the current study are available from the corresponding author upon reasonable request.

Conflicts of Interest: All authors was employed by the Automation Research and Design Institute of Metallurgical Industry Co., Ltd. The authors declare that the research was conducted in the absence of any commercial or financial relationships that could be construed as a potential conflict of interest.

References

1. Ohaeri, E.G.; Szpunar, J.A. An Overview on Pipeline Steel Development for Cold Climate Applications. *J. Pipeline Sci. Eng.* **2022**, *2*, 1–17. [CrossRef]
2. Pallaspuro, S.; Kaijalainen, A.; Mehtonen, S.; Komi, J.; Zhang, Z.; Porter, D. Effect of Microstructure on the Impact Toughness Transition Temperature of Direct-Quenched Steels. *Mater. Sci. Eng. A* **2018**, *712*, 671–680. [CrossRef]
3. Song, S.; Qin, G.; Lan, T.; Li, Z.; Xing, G.; Liu, Y. Study on Multi-Factor Coupling Fatigue Properties of Weathering Steel Welded Specimens. *Materials* **2025**, *18*, 4551. [CrossRef]
4. Wei, S.-H.; Lu, H.-C.; Liu, T.-S.; Wang, C.-C.; Xie, J.-X.; Dong, H. Effects of Rare Earth on Low Temperature Impact Toughness of HRB400E Rebar. *China Metall.* **2022**, *32*, 16–25.
5. Wang, Z.; Zeng, Q.; Wang, L.; Yao, Y.; Li, K. Corrosion of Rebar in Concrete under Cyclic Freeze–Thaw and Chloride Salt Action. *Constr. Build. Mater.* **2014**, *53*, 40–47. [CrossRef]
6. Wasudeo, K.A. Assessment of Fiber Optic Sensor Technologies for Real-Time Structural Health Monitoring of Civil Engineering Infrastructure. *J. Comput. Anal. Appl. (JoCAAA)* **2024**, *33*, 3489–3496.
7. Brownjohn, J.M.W. Structural Health Monitoring of Civil Infrastructure. *Philos. Trans. R. Soc. A* **2007**, *365*, 589–622. [CrossRef]

8. Soltani, E.; Ahmadi, E.; Gueniat, F.; Salami, M.R. A Review of Bridge Health Monitoring Based on Machine Learning. *Proc. Inst. Civ. Eng. Bridge Eng.* **2025**, *178*, 84–94. [CrossRef]
9. Sakaris, C.; Liu, Z.; Alamdari, M.; Schlanbusch, R. Direct and Indirect Structural Health Monitoring of Steel Railway Bridges: A State-of-the-Art Review and Future Challenges. *PHM Soc. Eur. Conf.* **2026**, *9*, 1–30. [CrossRef]
10. Milić, I.; Bleiziffer, J. Life Cycle Assessment of the Sustainability of Bridges: Methodology, Literature Review and Knowledge Gaps. *Front. Built Environ.* **2024**, *10*, 1410798. [CrossRef]
11. Chen, Q.; Wang, H.; Ma, X. Multi-Level Physics-Informed Neural Networks (ML-PINN): A Framework for Long-Term Atmospheric Corrosion Prediction. *Corros. Sci.* **2026**, *267*, 113902. [CrossRef]
12. Yu, X.; Wang, Q.; Khodadadi, N.; Nanni, A.; Mosalam, K.M. An Adaptive Bayesian Physics-Informed Neural Network Model for Predicting the Fatigue Life of High-Strength Steel under Non-Uniform Corrosion. *Comput.-Aided Civ. Infrastruct. Eng.* **2026**, *50*, 100112. [CrossRef]
13. Reichstein, M.; Camps-Valls, G.; Stevens, B.; Jung, M.; Denzler, J.; Carvalhais, N.; Prabhat, F. Deep Learning and Process Understanding for Data-Driven Earth System Science. *Nature* **2019**, *566*, 195–204. [CrossRef]
14. *GB/T 1499.2-2018*; Steel for the Reinforcement of Concrete—Part 2: Hot Rolled Ribbed Bars. Standards Press of China: Beijing, China, 2018.
15. *GB/T 229-2020*; Metallic Materials—Charpy Pendulum Impact Test Method. Standards Press of China: Beijing, China, 2020.
16. *YB/T 4368-2014*; Steel Bars Corrosion Test Method in Industrial Atmosphere Environment. Metallurgical Industry Press: Beijing, China, 2014.
17. *ASTM G101-04(2020)*; Standard Guide for Estimating the Atmospheric Corrosion Resistance of Low-Alloy Steels. ASTM International: West Conshohocken, PA, USA, 2020.
18. Tao, F.; Cheng, J.; Qi, Q.; Zhang, M.; Zhang, H.; Sui, F. Digital Twin-Driven Product Design, Manufacturing and Service with Big Data. *Int. J. Adv. Manuf. Technol.* **2018**, *94*, 3563–3576. [CrossRef]
19. He, Y.; Ma, Y.; Huang, K.; Wang, L.; Zhang, J. Digital Twin Bayesian Entropy Framework for Corrosion Fatigue Life Prediction and Calibration of Bridge Suspender. *Structures* **2025**, *82*, 110711.
20. Wang, T.; Li, D.; Li, B.; Zhang, J. Lightweight Structural Health Monitoring Method for Bridges Based on Cloud-Edge Collaborative Optimization. *Structures* **2025**, *80*, 109954. [CrossRef]
21. Frangopol, D.M.; Soliman, M. Life-Cycle of Structural Systems: Recent Achievements and Future Directions. *Struct. Infrastruct. Eng.* **2016**, *12*, 1–20. [CrossRef]
22. Feng, Z.; Jiang, Z.; Yan, C. Prediction of Corrosion Lifetime of Marine Environment Steel Pipe Piles Based on Physics-Informed Neural Network. *Discov. Appl. Sci.* **2025**, *8*, 136. [CrossRef]
23. Oldfield, W. Fitting Curves to Toughness Data. *J. Test. Eval.* **1979**, *7*, 326–333. [CrossRef]
24. Jones, D.A. *Principles and Prevention of Corrosion*, 2nd ed.; Prentice Hall: Upper Saddle River, NJ, USA, 1996.
25. Guo, X.-Y.; Fang, S.-E.; Zhu, X.; Li, J. A Semi-Markov Process Based Digital Twin for Safety Evaluation of Cable-Stayed Bridges with Cable Corrosion. *Adv. Eng. Inform.* **2025**, *65*, 103270. [CrossRef]
26. Li, X.; Fu, Z.; Guo, H.; Ji, B.; Xu, Z. A Closed-Loop Framework Integrating Robotic Inspection and Digital Twins for Fatigue Prognosis of In-Service Steel Bridges. *Commun. Eng.* **2026**, *10*, 76. [CrossRef]
27. Karpatne, A.; Atluri, G.; Faghmous, J.H.; Steinbach, M.; Banerjee, A.; Ganguly, A.; Shekhar, S.; Samatova, N.; Kumar, V. Theory-Guided Data Science: A New Paradigm for Scientific Discovery from Data. *IEEE Trans. Knowl. Data Eng.* **2017**, *29*, 2318–2331. [CrossRef]
28. Lu, N.; Wang, K.; Wang, H.; Liu, X.F.; Luo, Y. Real-Time Fatigue Crack Detection and Prediction in Steel Structures Based on an Automated Digital Twin-Driven Framework. *Thin-Walled Struct.* **2025**, *218*, 114099. [CrossRef]
29. Yang, L.; Zhang, X.; Liu, Y.; Chen, Z. Edge Computing-Enabled Digital Twin for Real-Time Structural Health Monitoring of Bridges. *Autom. Constr.* **2025**, *172*, 106023.
30. Grieves, M.; Vickers, J. Digital Twin: Mitigating Unpredictable, Undesirable Emergent Behavior in Complex Systems. In *Transdisciplinary Perspectives on Complex Systems*; Springer: Cham, Switzerland, 2017; pp. 85–113.
31. *GB/T 228.1-2021*; Metallic Materials—Tensile Testing—Part 1: Method of Test at Room Temperature. Standards Press of China: Beijing, China, 2021.
32. Zhang, X.-B.; Cui, C.; Zhang, Q.-H.; Li, Y.-P. Thermodynamic Entropy Based Low-Temperature Fatigue Life Prediction for Q500qENH Weathering Steel in Bridges. *Case Stud. Constr. Mater.* **2024**, *21*, e04029. [CrossRef]
33. Cheng, D.; Lv, B.; Chen, C.; Yang, Z.; Hao, X.; Zheng, C.; Zhang, F. Synergistic Mechanism of Minor Ni and Cr to Enhance the Corrosion Resistance of Novel Pearlitic Rail Steel. *Constr. Build. Mater.* **2025**, *484*, 141846. [CrossRef]
34. Mizan, M.H.; Hayakawa, R.; Matsumoto, K. Effects of Combined Deterioration of Steel Corrosion and Freeze-Thaw Cycles on the Pull-Out Behavior of Deformed Bars in Concrete. *Constr. Build. Mater.* **2025**, *505*, 144758. [CrossRef]
35. Melchers, R.E.; Beck, A.T. *Structural Reliability Analysis and Prediction*, 2nd ed.; John Wiley & Sons: Hoboken, NJ, USA, 2018.

36. Zhang, X.; Fan, C.; Yang, J.; Yong, Z. Adaptive Compensated MUSIC Beamforming for Lamb Wave Damage Localization under Varying Temperature. *Struct. Health Monit.* **2026**, *OnlineFirst*. [CrossRef]
37. Rezazadeh, N.; De Luca, A.; Lamanna, G.; Annaz, F.; de Oliveira, M. A Novel Interpretable Domain Adaptive Framework for Robust Damage Detection in Composite Structures under Environmental Variability. *Struct. Health Monit.* **2026**, *OnlineFirst*. [CrossRef]
38. Nasim, M.; Sarteshnizi, I.T.; Rajabifard, A.; Samali, B. Evolving Research Directions toward Practical Bridge Health Monitoring with Streaming Data. *J. Infrastruct. Intell. Resil.* **2026**, *5*, 100226. [CrossRef]
39. Buka-Vaivade, K.; Nicoletti, V.; Gara, F. Advancing Bridge Resilience: A Review of Monitoring Technologies for Flood-Prone Infrastructure. *Open Res. Eur.* **2025**, *5*, 26. [CrossRef]
40. Straub, D.; Der Kiureghian, A. Combining Bayesian Networks with Structural Reliability Methods: Application to Corrosion of Reinforcing Steel. *Reliab. Eng. Syst. Saf.* **2011**, *96*, 814–824.
41. Kim, S.; Kim, H.; Hwang, Y. Data-Driven Dynamic Response Forecasting and Anomaly Detection in Long-Span Bridges. *J. Civ. Struct. Health Monit.* **2025**, *15*, 3045–3062. [CrossRef]
42. Raharjo, N.D. Bridge Monitoring Health Using Advanced Technology: A Systematic Review. *IOP Conf. Ser. Earth Environ. Sci.* **2025**, *1551*, 012069. [CrossRef]
43. Mammeri, S.; Barros, B.; Conde-Carnero, B.; Riveiro, B. From Traditional Damage Detection Methods to Physics-Informed Machine Learning in Bridges: A Review. *Eng. Struct.* **2025**, *327*, 119862. [CrossRef]
44. Bao, Y.; Sun, H.; Xu, Y.; Guan, X.; Pan, Q.; Liu, D. Recent Advances in Structural Health Diagnosis: A Machine Learning Perspective. *Adv. Bridge Eng.* **2025**, *6*, 7. [CrossRef]
45. Alves, R.; Lousada, S.; Jankauskienė, D.; Pukite, V. A Data-Driven Strategy for the Structural Health Monitoring of the Machico Cable-Stayed Bridge: A Case Study. *Buildings* **2025**, *15*, 4150. [CrossRef]
46. Liu, H.; Liu, M.; Yang, G.; Dai, X.; Shen, Y.; Liang, B.; Ding, X.; Xu, Y.; Wang, R. Research on Precursory Warning of Damage and Failure in Freeze-Thaw Sandstone Based on Acoustic-Thermal Joint Monitoring. *Cold Reg. Sci. Technol.* **2025**, *228*, 104679. [CrossRef]
47. Zhu, L.; Su, R.K.-L.; Ma, J.-J.; Ni, Y.-J. Experimental Case Study on the Fatigue Behavior of Steel–Concrete Composite Beams after Chloride-Induced Corrosion and Cyclic Freeze–Thaw. *J. Bridge Eng.* **2023**, *28*, 05022012. [CrossRef]

Disclaimer/Publisher's Note: The statements, opinions and data contained in all publications are solely those of the individual author(s) and contributor(s) and not of MDPI and/or the editor(s). MDPI and/or the editor(s) disclaim responsibility for any injury to people or property resulting from any ideas, methods, instructions or products referred to in the content.